Desalination and Water Treatment
www.deswater.com

doi: 10.5004/dwt.2022.28897

276 (2022) 13–27
November

Sensitivity analysis of double slope solar still having compound parabolic concentrator integrated ETCs by incorporating heat transfer coefficients, exergy gain and exergy efficiency

Ajay Raj Singh[a], Alka Bani Agarwal[a], Desh Bandhu Singh[b,*]

[a]*Department of Mechanical Engineering, UIT, RGPV, Bhopal-462033, M.P., India, email: ajayraj.sliet2k3@gmail.com (A.R. Singh), alk_agr11@yahoo.in (A.B. Agarwal)*

[b]*Department of Mechanical Engineering, Graphic Era Deemed to be University, Bell Road, Clement Town, Dehradun – 248002, Uttarakhand, India, email: dbsiit76@gmail.com/Deshbandhusingh.me@geu.ac.in (D.B. Singh)*

Received 11 February 2022; Accepted 4 September 2022

ABSTRACT

This work presents a sensitivity analysis of double slope solar still having N similar compound parabolic concentrator integrated evacuated tubular collectors in series connection (NCPCETC-DS) by incorporating heat transfer coefficient, exergy gain and exergy efficiency using one-at-a-time method. The sensitivity investigation for collector has also been done. All expressions of various parameters have been fed to computational code developed in MATLAB – 2015a for May month of New Delhi climatic situation. Heat transfer coefficients, exergy gain and exergy efficiency values have been estimated for different cases in which one input variable is varied keeping other input parameters as constant and the computation is continued till the completion of estimation for all input parameters. The exergy gain for collector, exergy gain for NCPCETC-DS and exergy efficiency for NCPCETC-DS have been estimated to be most sensitive with regard to concentration ratio having mean sensitivity figure values as 1.88, 1.97 and 1.94 in that order.

Keywords: Sensitivity investigation; CPCETC; Double slope solar still; Exergy; Efficiency

1. Introduction

The solar still is a box type structure containing condensing surface at the top for allowing the solar energy to enter the basin and further permitting the condensation of water vapor which trickles down to the channel from where water is siphoned off. It imitates natural hydrological cycle and the working of solar still is based on greenhouse effect. It is simple and environmentally friendly. Locally available materials can be used for its construction, and it has the great potential to mitigate the contemporary issue of water scarcity. However, it is bulky, it requires high initial investment and technicians are not available at local level. The solar still is broadly divided into passive and active solar stills. The passive solar still does not receive heat from an ancillary unit like solar collectors, however, it suffers from the low output issue which can be overcome by supplying heat from auxiliary unit to passive solar still for increasing the temperature of water in the basin. Due to increased temperature difference between water surface and condensing cover, an enhanced water yield is obtained. When heat is supplied to passive solar still, it becomes active solar still. Both passive and active solar stills are further categorized as single slope and double slope solar stills.

The investigation of double slope solar still having concentrator collectors is the requirement of contemporary situation because conventional source of energy is very limited and solar still which solely works on solar energy has the

* Corresponding author.

potential to mitigate the issue of freshwater lack prevailing all over the world. The solar still working in active mode was reported in 1983 [1] and a lot of advancements have been reported throughout the world by researchers. Further, two flat plate collectors (FPCs) in which one FPC was integrated with photovoltaic thermal (PVT) [2] were included with single slope solar still (SS) because PVT integrated collectors provide better electrical efficiency as reported by Kern and Russell [3]. The thermal energy collected by water flowing below PVT is utilized in heating water in the basin of SS. Moreover, the extension of Kumar and Tiwari [2] work was done for double slope solar still (DS) [4]. An investigation on SS by incorporating PVTFPCs was done in which both collectors were identical [5,6]. It was stated that the electrical energy output was higher; however, thermal energy was lower than the corresponding values for similar system reported earlier [2]. An optimization of mass-flow-rate and number of collectors [7–11] considering the boiling of water at NTP as constraint was done for estimation of various parameters of an active solar still. A study consisting of the effect of nanoparticles on the performance of DS working in active mode was done by Sahota and Tiwari [12], Carranza et al. [13] and Kouadri et al. [14]. They reported an improved performance of active solar still if nanoparticles were mixed with base fluid due to improved thermophysical property. Kandeal et al. [15] studied double slope solar still with modification and it was concluded that the saving in freshwater production cost was 35.5% over conventional solar still when nanofluid in combination with phase change material was used. It occurred due to improved thermophysical characteristic of fluid. Thakur et al. [16] studied solar still loaded with nanofluid in combination with solar absorber and an improvement in potable water yield of 39.3% over conventional solar still was reported due to high thermal conductivity and good solar absorption capability of activated carbon nanoparticles based solar absorber. Tyagi et al. [17] reviewed photovoltaic systems loaded with nanofluid and it was concluded that nanofluids enhanced the efficiency of systems due to the improvement in physiothermal characteristics.

Atheaya et al. [18] investigated FPC by incorporating parabolic concentrating surfaces keeping in mind that the resulting collector could perform better due to the concentration of solar intensity on the receiver surface. It was further extended by Tripathi et al. [19] for a number (N) of collectors in open loop. An investigation of basin type solar still having concentrating collectors was done [20–27]. They reported the analytical equation development and concluded that DS in active mode performed better than SS in active mode because of more uniform allocation of solar intensity in the case of DS at 280 kg water mass in the basin. The sensitivity investigation for DS working in active mode was carried out and it was stated that this type of investigation might help a lot to the designer and installer of such systems because of having knowledge about the influence of input parameters on the performance in advance [28–30]. Raturi et al. [31,32] studied sensitivity analysis of basin type solar still and they concluded that this type of analysis helps a lot to the designer and installer of basin type solar still as it gives the information regarding the significance of input parameter on output parameter.

A further improvement in the performance of collector and hence solar still was felt by preventing loss by convection. Keeping it in mind, an evacuated tubular collector (ETC) was developed and it was integrated with solar still to know the effect of preventing heat loss by convection on its output. Similar investigation on solar still by including ETCs was done [33–35] and an improved performance of solar still working in active mode over similar solar still working in passive mode was reported. An analytical equation development for ETC was done by Mishra et al. [36] which his work was carried forward by integrating basin type solar still with ETCs under optimized situation and it was reported that DS working in active mode performed better than SS working in active mode at 280 kg of water mass in the basin due to better dispersal of solar energy in DS [37–39]. Issa and Chang [40] investigated SS having ETCs in mixed connection experimentally and it was reported that SS in active mode performed better than passive mode due to the supply of heat to basin of active mode operated solar still. Analytical equations for solar still by incorporating ETC as well as ETC integrated concentrators separately were developed, and a comparative study was done based on energy metrics [41–44]. Solar still incorporated with ETC integrated concentrators performed better than the solar still integrated with ETC due to having better heat addition capability of ETC integrated concentrators to the basin of solar still. Sharshir et al. [45] studied solar still by keeping three different materials on the water surface for enhancing the performance by minimizing heat loss and concluded that the highest increase in yield output was 51.8% over conventional solar still. Thakur et al. [46] have studied solar still using various augmentation technique experimentally and it was concluded that the solar still registered an enhancement of 58.15% and 64.44% when reduced graphene oxide coated absorber plate along with porous activated carbon over conventional solar still.

A review of solar still included with various kinds of collectors has been reported by Patel et al. [47–49]. A review of solar still included with various kinds of collectors using nanoparticles has been reported by Singh et al. [50] and it was concluded that active solar still using nanoparticles performed better due to having improved thermophysical properties of fluid upon addition of nanoparticles. A short review on the effect of various kinds of materials for absorber has been reported by Bansal et al. [51]. Mourad et al. [52] reviewed the various solar collectors with phase change materials and Said et al. [53] have reviewed solar collectors loaded with nanofluid. Shankar et al. [54] studied solar still included with ETC in natural and forced modes and it was concluded that the performance was better in the case of forced mode due to higher amount of supply of heat to basin. An investigation on spherical and pyramid solar stills was carried out by Abdallah et al. [55] and it was concluded that spherical shaped system performed better due to more effective utilization of solar energy in the case of spherical shaped solar still. Sharma et al. [56] carried out experimental validation of SS active solar still and it was reported that the correlation coefficient for yield was 0.9951. Purnachandrakumar et al. [57] have reviewed on the application of computational fluid dynamics (CFD) concept to different solar stills and concluded that CFD is a cost-effective tool for the simulation of solar still. Kumar et al. [58] have reviewed the basin type solar still by incorporating evacuated tubular collectors. Kumar et al. [59] studies the effect of variation of water depth on the performance of solar still. Yadav et al. [60] studied the effect of variation of mass flow rate and number of collectors on yearly overall energy as well as exergy and it was concluded that the output decreases with the increase in mass flow rate because water passing through collectors get less time for absorption of heat at increased value of mass flow rate and less heat is added to basin. Singh et al. [61–63] studied the effect of variation of mass flow rate and N on the performance of solar still and they concluded that the output of solar still got diminished with the increase in mass flow rate and the reverse occurred with the increase in Thakur and Sathyamurthy [64] studied tubular solar still with eggshell powder as sensible heat storage material experimentally and it was concluded that the cost of potable water produced was reduced by 47.62% as compared to tubular solar still without eggshell powder.

From the existent literature review, one can observe that the sensitivity analysis of double slope solar still having compound parabolic concentrator integrated ETCs (NCPCETC-DS) by incorporating heat transfer coefficients, exergy gain and exergy efficiency has not been carried out by any researcher throughout the globe. This type of analysis for NCPCETC-DS will help the designer and installer in deciding the level of different input parameters while designing such system from exergy viewpoint. Hence, the proposed research deals with the sensitivity investigation of NCPCETC-DS by incorporating exergy gain and exergy efficiency. The main objects the research work can be written as:

- To inspect outcomes of NCPCETC and NCPCETC-DS by differing mass flow rate (MFR) to know its influence on exergy output and exergy efficiency keeping other input parameters constant.
- To examine outcomes of CPCETC and NCPCETC-DS by differing N to know its influence on exergy output and exergy efficiency for given values of MFR, concentration ratio (CR) and water depth (WD).
- To check the effect of variation in WD on exergy output and exergy efficiency for CPCETC as well as NCPCETC-DS considering other input parameters constant.
- To estimate the effect of changing CR on exergy output and exergy efficiency for CPCETC as well as NCPCETC-DS at given values of all other input parameters.
- To compare performance parameters based on average values of sensitivity figures (SFs).

2. System description

The arrangement of different components of the system has been depicted as Fig. 1 and cut section of one collector has been depicted as Fig. 2. Here, CPCETCs have been arranged in series with an objective of realizing elevated temperature of fluid at the exit of last CPCETC. The solar still of double slope in active mode has been oriented east–west to get maximum annual energy for New Delhi location. The specification of NCPCETC-DS has been presented in Table 1. When solar energy impinges on the system, fluid passing through collectors gains heat from the solar energy and transfers the same to water in the basin of DS. The solar intensity falling on the surface of DS gets reflected first and then absorbed by the condensing surface and the remaining part (approximately 95%) is transmitted to water in the basin. Again, some part of intensity is

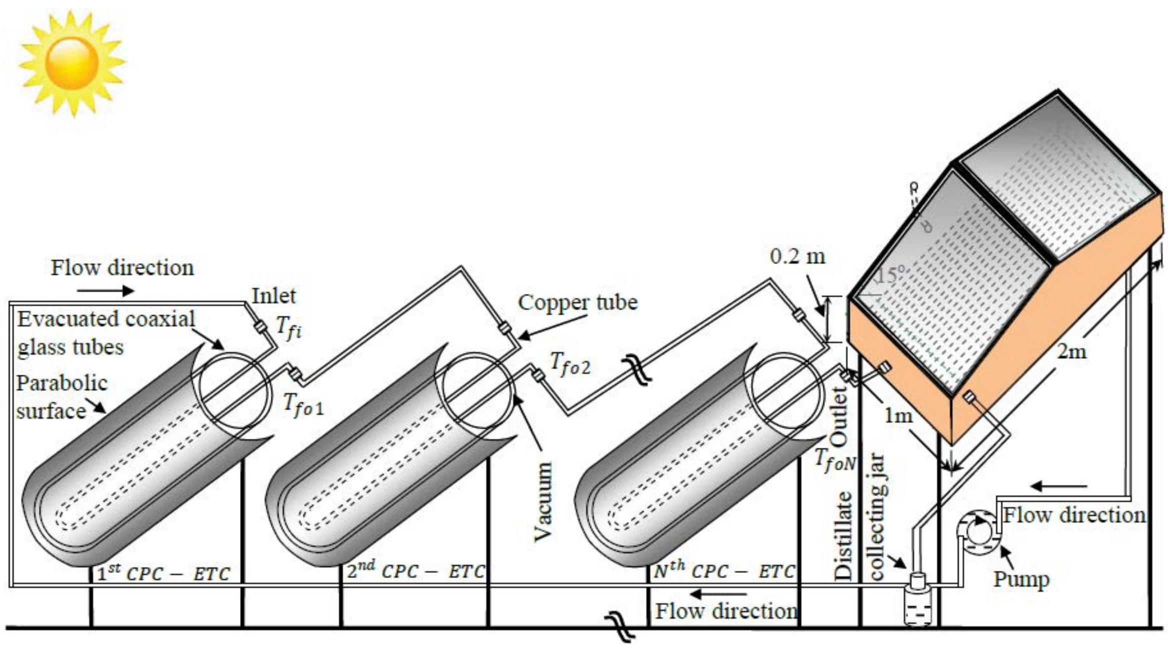

Fig. 1. N identical CPCETCs integrated double slope solar distiller unit (NCPCETC-DS).

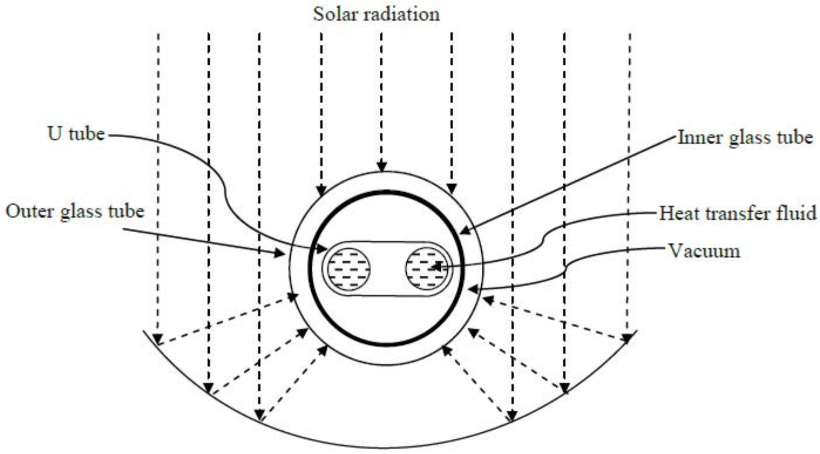

Fig. 2. Cross-section side view of the first CPCETC.

Table 1
Specification of NCPCETC-DS

Component	Specification	Component	Specification
Double slope active solar still			
Length	2 m	Cover material	Glass
Width	1 m	Orientation	East–west
Inclination of glass cover	15°	Thickness of glass cover	0.004 m
Height of smaller side	0.2 m	K_g	0.816 W/m-K
Material of body	GRP	Thickness of insulation	0.1 m
Material of stand	GI	K_i	0.166 W/m-K
CPCETC			
Type and no. of collectors	ETC, N	α_p	0.8
DC motor rating	12 V, 24 W	F'	0.968
Radius of inner copper tube	0.0125 m	τ_g	0.95
Thickness of copper tube	0.0005 m	K_g (Wm/K)	1.09
Outer radius of outer glass tube of evacuated coaxial glass tube	0.024 m	Angle of ETC with horizontal	30°
Inner radius of inner glass tube of evacuated coaxial glass tube	0.0165 m	Length of each copper Tube	2.0 m
Thickness of outer/inner glass tube of evacuated coaxial glass tube	0.002 m	CR	2

reflected by water, some part is absorbed by water and the remaining part is transmitted to the blackened surface at the bottom (basin liner); where, almost all solar radiation gets absorbed by the surface resulting in the increase in temperature of the blackened surface. The temperature of this surface becomes even higher than water and heat in turn is transferred to water from basin liner. In this way, water receives heat from NCPCETCs, directly from sunlight and indirectly from basin liner resulting in the increase in temperature of water which generates a difference of temperature between water surface and condensing surface. This difference of temperatures compels water to evaporate. The vapor gets condensed at the inner side of glass through film-wise condensation and trickles down to the channel fixed at lower sides from where freshwater is siphoning off and collected in the measuring jar.

3. Thermal model for NCPCETC-DS

The relation for heat gained by NCPCETCs and the expression for temperature of outcoming fluid (water) can be expressed as [36].

$$\dot{Q}_{\mathrm{uN}} = \left(\mathrm{PF}_1\right)\left(\alpha\tau\right)_{\mathrm{eff}} \frac{\left(1-K_k^N\right)}{\left(1-K_k\right)} I_b\left(t\right) - \left(A_r F_r\right) U_L \frac{\left(1-K_k^N\right)}{\left(1-K_k\right)}\left(T_{\mathrm{fi}}-T_a\right) \quad (1)$$

$$T_{\text{foN}} = \frac{\text{PF}_1(\alpha\tau)_{\text{eff}}(A_rF_r)}{\dot{m}_fC_f}\frac{(1-K_K^N)}{(1-K_K)}I_b(t) + \frac{(A_rF_r)U_L}{\dot{m}_fC_f}\frac{(1-K_K^N)}{(1-K_K)}T_a + K_K^NT_{\text{fi}} \tag{2}$$

Here, all unknown terms present in Eqs. (1) and (2) are available in Appendix of Sharma et al. [44].

Following Sharma et al. [43,44], the mathematical relations for numerous elements of DS can be composed; and using Eqs. (1) and (2), equations for different components so obtained can be simplified for getting water temperature (T_w), temperature at inside surface of glass towards east (T_{giE}) and temperature at inside surfaces of glass towards west (T_{giW}) as follows:

$$T_w = \frac{\overline{f}(t)}{a}\left(1-e^{-\text{at}}\right) + T_{w0}e^{-\text{at}} \tag{3}$$

$$T_{\text{giE}} = \frac{A_1 + A_2T_w}{P} \tag{4}$$

$$T_{\text{giW}} = \frac{B_1 + B_2T_w}{P} \tag{5}$$

Again, all unknown terms present in Eqs. (3) and (4) have been given in Appendix-A. After evaluating the values of T_w and T_{gi} from Eqs. (5) and (6) in that order, the value of hourly exergy gain can be estimated as [65]:

$$\dot{\text{E}}\text{x} = h_{\text{ewg}} \times \frac{A_b}{2}\left[\begin{array}{l}\left\{\left\{\left(T_w - T_{\text{giE}}\right) + \left(T_a + 273\right)\ln\left(\dfrac{T_w + 273}{T_{\text{giE}} + 273}\right)\right\}\right\} \\ +\left\{\left(T_w - T_{\text{giW}}\right) + \left(T_a + 273\right)\ln\left(\dfrac{T_w + 273}{T_{\text{giW}} + 273}\right)\right\}\end{array}\right] \tag{6}$$

Evaporative heat transfer coefficient (HTC) from water surface to the condensing glass surface can be calculated as:

$$h_{\text{ewgE}} = 16.273 \times 10^{-3} h_{\text{cwgE}}\left[\frac{P_w - P_{\text{giE}}}{T_w - T_{\text{giE}}}\right] \tag{7}$$

$$h_{\text{ewgW}} = 16.273 \times 10^{-3} h_{\text{cwgW}}\left[\frac{P_w - P_{\text{giW}}}{T_w - T_{\text{giW}}}\right] \tag{7a}$$

Here, $h_{\text{cwgE}} = 0.884\left[\left(T_w - T_{\text{giE}}\right) + \frac{\left(P_w - P_{\text{giE}}\right)\left(T_w + 273\right)}{\left(268.9 \times 10^3 - P_w\right)}\right]$ (8)

$$h_{\text{cwgW}} = 0.884\left[\left(T_w - T_{\text{giW}}\right) + \frac{\left(P_w - P_{\text{giW}}\right)\left(T_w + 273\right)}{\left(268.9 \times 10^3 - P_w\right)}\right] \tag{8a}$$

$$P_w = \exp\left[25.317 - \frac{5,144}{\left(T_{\text{giE}} + 273\right)}\right] \tag{9}$$

$$P_{\text{giE}} = \exp\left[25.317 - \frac{5,144}{\left(T_{\text{giE}} + 273\right)}\right] \tag{10}$$

$$P_{\text{giW}} = \exp\left[25.317 - \frac{5,144}{\left(T_{\text{giW}} + 273\right)}\right] \tag{10a}$$

The radiative HTCs between water surface and east oriented as well as west oriented glass covers can be written as:

$$h_{\text{rwE}} = \left(0.82 \times 5.67 \times 10^{-8}\right)\left[\left(T_w + 273\right)^2 + \left(T_{\text{giE}} + 273\right)^2\right]\left[T_w + T_{\text{giE}} + 546\right] \tag{11}$$

$$h_{\text{rwW}} = \left(0.82 \times 5.67 \times 10^{-8}\right)\left[\left(T_w + 273\right)^2 + \left(T_{\text{giW}} + 273\right)^2\right]\left[T_w + T_{\text{giW}} + 546\right] \tag{12}$$

HTC between water surface and east oriented glass cover as well as west oriented glass covers can be written as:

$$h_{1E} = h_{\text{ewgE}} + h_{\text{cwgE}} + h_{\text{rwE}} \tag{13}$$

$$h_{1W} = h_{\text{ewgW}} + h_{\text{cwgW}} + h_{\text{rwW}} \tag{14}$$

HTC between east and west oriented glass covers can be estimated as:

$$h_{\text{EW}} = 0.034 \times 5.67 \times 10^{-8}\left[\left(T_{\text{giE}} + 273\right)^2 + \left(T_{\text{giW}} + 273\right)^2\right]\left[T_{\text{giE}} + T_{\text{giW}} + 546\right] \tag{15}$$

The total HTC between water surface and glass cover can be estimated as:

$$h_1 = h_{1E} + h_{1W} \tag{16}$$

Total evaporative HTC between water surface and glass cover can be estimated as:

$$h_e = h_{\text{ewgE}} + h_{\text{ewgW}} \tag{17}$$

The value of hourly exergy gain for NETCs can be estimated as:

$$\dot{\text{E}}\text{x}_c = \dot{m}_fC_f\left[\left(T_{\text{foN}} - T_{\text{fi}}\right) + \left(T_a + 273\right)\ln\left(\frac{T_{\text{foN}} + 273}{T_{\text{fi}} + 273}\right)\right] \tag{18}$$

The daily exergy can be estimated as addition of per hour exergy for 24 h.

Hourly and daily exergy efficiencies for NCPCETC-DS ($\eta_{\text{NCPCETC-DS}}$) can be estimated as follows [17]:

$$\eta_{\text{NCPCETCDS,hourly}} = \frac{\dot{\text{E}}\text{x}}{\left[\begin{matrix}\dot{\text{E}}\text{x}_c + \left[0.933 \times \left\{\frac{A_b}{2}\left(I_{\text{SE}} + I_{\text{SWE}}\right)\right\}\right] \\ +\text{pump work}\end{matrix}\right] \times 3{,}600} \tag{19}$$

$$\eta_{\text{NCPCETCDS,daily}} = \frac{\sum_1^{24} \dot{\text{E}}\text{x}}{3{,}600 \times \sum_1^{10} \left[\begin{matrix}\dot{\text{E}}\text{x}_c + \left[\begin{matrix}0.933 \times \\ \left\{\frac{A_b}{2}\left(I_{\text{SE}} + I_{\text{SWE}}\right)\right\}\end{matrix}\right] \\ +\text{pump work}\end{matrix}\right]} \times 100 \tag{20}$$

The several terms used in Eqs. (1–19) are available in appendix of Sharma et al. [38,39].

4. Sensitivity analysis for NCPCETC-DS

Sensitivity analysis deals with the effect of variation of input parameter on output parameter under certain assumptions. There are many ways of performing sensitivity analysis; however, one-at-a-time (OAT) method is simple and most popular. This type of analysis provides information to the designer and installer of the system about the significance of input parameter with respect to output parameter. In other words, which parameter affect output most is known which help them to focus on particular parameter under the aim of getting particular output as per the need of the customer. Sensitivity analysis also measures the robustness of the system. It helps in understanding the deep relationship which exists between output and input parameters. The quantization of the sensitivity can be done with the help of sensitivity figure (SF) which can be written as:

$$\text{SF} = \frac{\text{Percentage chance in output parameter}}{\text{Percentage change in input parameter}} \tag{21}$$

Using sensitivity analysis, criticality of parameters can be determined and can be arranged in either increasing or decreasing order in terms of criticality of parameter of the system. A detailed information is available to the modeler or designer about which parameter is most critical followed by other parameters [66,67]; it may be one of the reasons for carrying out the sensitivity analysis. OAT method of carrying out sensitivity analysis consists of estimating the effect on output parameter by varying one parameter keeping other input parameters fixed. It is continued till the calculation is accomplished for all input parameters of the system. The system with different input and output parameters has been presented schematically as Fig. 3. Out of all input parameters shown in Fig. 3, wind velocity, solar flux and atmospheric temperature has not been considered for the sensitivity analysis estimation because these parameters are exceedingly reliant on weather situation; the study of the remaining input parameters have been carried out and they have been discussed in the present analysis. Ajbar et al. [68] reported the use of artificial neural network and multiple linear regression model for knowing the effect of input parameters on the outlet temperature of parabolic trough collector and it was concluded that the artificial neural network is more suitable for simulating and optimizing the outlet temperature of parabolic trough collector. Recently, Ajbar et al. [69] have reported the comprehensive review on parabolic trough collector and it has been concluded that the application of nanofluids with turbulators resulted in the best option for improving the performance of parabolic trough collector.

5. Solution procedure

The solution procedure regarding sensitivity analysis for NCPCETC-DS can be stated as:

Step I

All required data has been accessed from IMD, Pune, India. The expression given by Liu and Jordan has been employed for the estimation of solar intensity on the inclined surface using computing code in MATLAB-2015a.

Step II

Values of different HTCs have been computed using Eqs. (7)–(17). Values of different temperatures namely T_w, T_{giE} and T_{giW} have been computed using Eqs. (3)–(5) respectively.

Step III

Values of exergy gain and exergy efficiency have been evaluated for different values of one input parameter

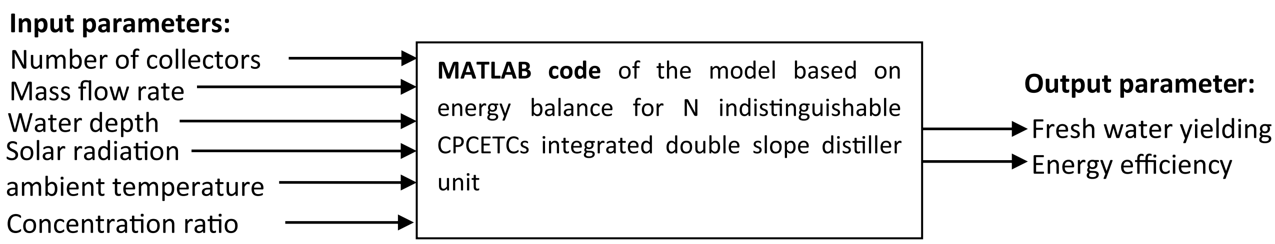

Fig. 3. Purification of saline/brackish water to potable water using NCPCETC-DS.

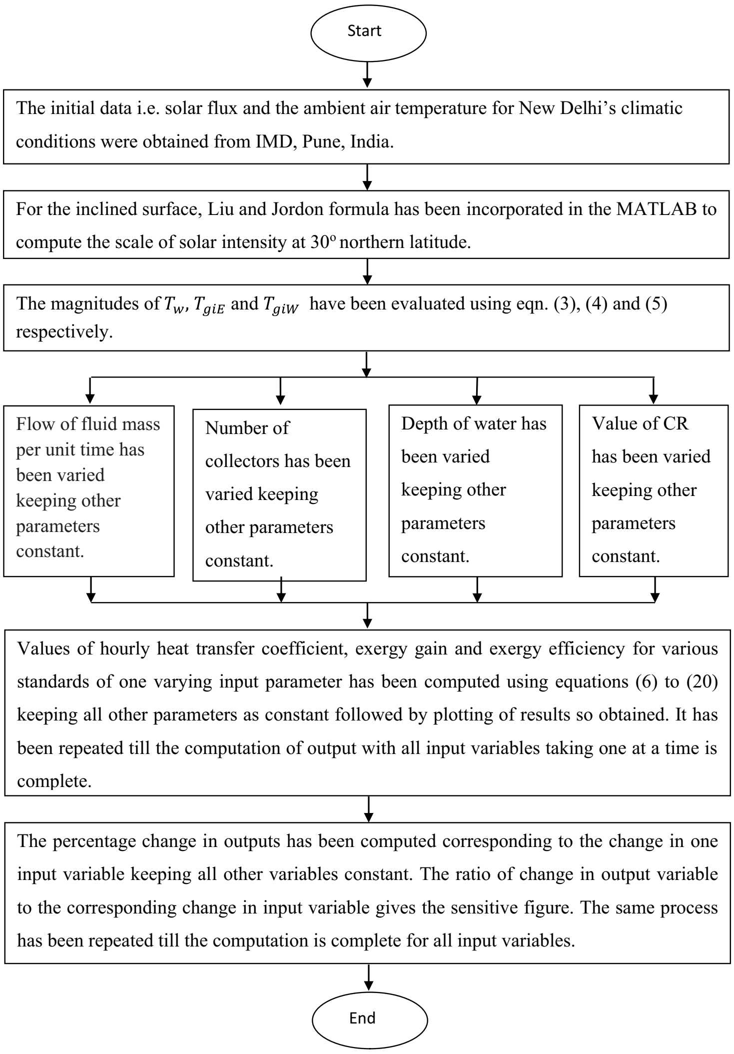

Fig. 4. Flow chart of methodology for carrying out sensitivity analysis for NCPCETC-DS.

keeping other input parameters constant. It is repeated till the evaluation for all parameters is completed.

Step IV

Results obtained in Step-III has been plotted and percentage change in output parameters and percentage change in input parameters followed by the evaluation of sensitivity figure for each variable under consideration.

Step V

Comparison of sensitivity figures has been done.

The adopted solution procedure for carrying out sensitivity analysis has been depicted as flow chart in Fig. 4 with an objective of better understanding of methodology followed.

6. Results and discussion

All input parameters of NCPCETC-DS have been made input to computing code developed in MATLAB-2015a for carrying sensitivity investigation of NCPCETCs and NCPCETC-DS separately. Fig. 5 indicates the variation of solar flux and atmospheric temperature. Input data presented in Fig. 5 have been accessed from IMD, Pune, India. Outputs from the computing code have been presented as Figs. 6–21. OAT has been employed for sensitivity analysis of NETCs as well as NCPCETC-DS.

The dissimilarity in daily HTCs with MFR for NCPCETC-DS keeping all other input parameters persistent has been revealed as Fig. 6. One can observe from Fig. 6 that there is a sharp decrease in values of evaporative, radiative and total HTCs initially and then become almost constant after certain value of MFR. The reason being that the fluid passing through collectors does not get sufficient time to extract heat from solar energy and this tendency becomes more prominent at increased values of MFR. Lesser heat absorption means lower heat addition to basin and lower rise in temperature of water. Higher the speed of flow of fluid through collectors, lesser the time available for absorption of heat which results in lower amount of heat addition to basin and ultimately lower values of HTCs are obtained as HTCs are dependent on temperature of water.

The variation in daily HTCs with N for NCPCETC-DS keeping all remaining input parameters constant has been depicted as Fig. 7. One can see in Fig. 7 that values of evaporative, radiative and total HTCs increase with the enhancement in value of N keeping other input parameters constant. The reason being that the amount of heat supply to basin gets enhanced with increased value of N and elevated temperature of water is obtained which ultimately results in the increase in values of HTCS. The variation in daily HTCs with WD for NCPCETC-DS keeping all other input parameters persistent has been depicted as Fig. 8. One can see in Fig. 8 that values of evaporative, radiative and total HTCs increases with the increase in value of WD keeping other input parameters constant. The reason being that the amount of sensible heat storage during daytime increases with the increase in WD and this sensible heat contributes to increased temperature of water during night time which ultimately results in the increase in values of HTCS. The variation of daily HTCs with CR for NCPCETC-DS keeping all other input parameters as persistent has been depicted as Fig. 9. One can see in Fig. 9 that values of evaporative, radiative and total HTCs enhances with the enhancement in value of CR keeping all other input parameters persistent. The reason being that the amount of heat supply to basin gets enhanced with increased value of CR because more solar intensity is focused on receiver surface and enhanced water temperature is obtained which ultimately results in the increase in values of HTCS.

Sensitivity of daily HTC with regard to (a) MFR, (b) N, (c) WD and (d) CR for NCPCETC-DS has been revealed as Fig. 10. One can see that value of sensitivity figures in Fig. 10a–c decreases sharply at higher values of percentage change in input parameters; however, change in sensitivity figure becomes less at lower values of percentage change in input parameters because of similar trends in slope of

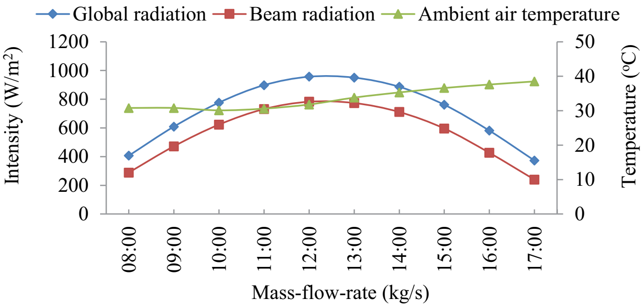

Fig. 5. Hourly variation of intensity and ambient air temperature for a typical day in the month of May.

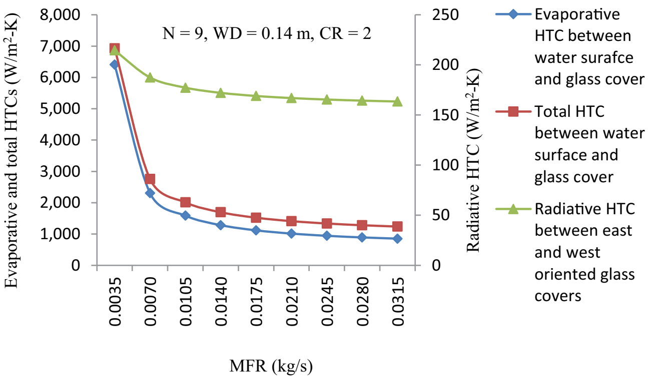

Fig. 6. Dissimilarity of daily heat transfer coefficients (HTCs) with MFR at selected values of N, CR and WD for NCPCETC-DS.

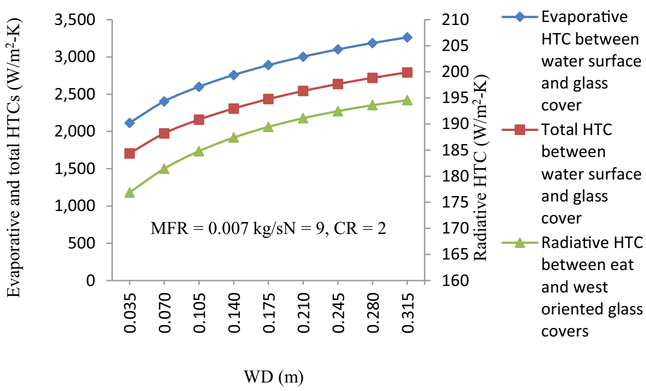

Fig. 8. Dissimilarity of daily heat transfer coefficients (HTCs) with WD at selected values of N, CR and MFR for NCPCETC-DS.

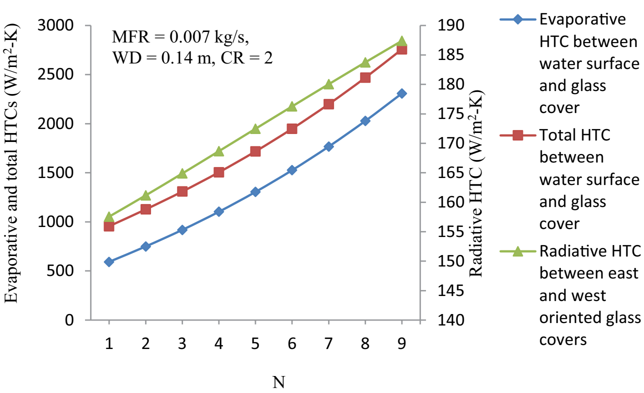

Fig. 7. Dissimilarity of daily heat transfer coefficients (HTCs) with N at selected values of MFR, CR and WD for NCPCETC-DS.

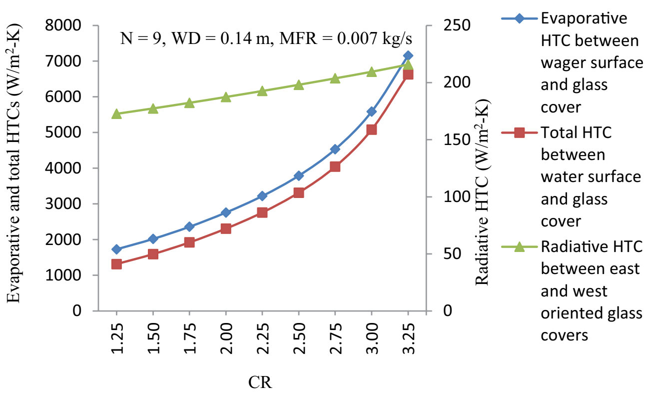

Fig. 9. Dissimilarity of daily heat transfer coefficients (HTCs) with CR at selected values of N, CR and MFR for NCPCETC-DS.

curves. Further, the change in sensitivity figure is relatively low with respect to WD as depicted in Fig. 10c. The mean value of sensitivity figure (SF) has been estimated to be 1.88, 1.58, 0.32 and 0.07 with respect to CR, N, MFR and WD respectively. It means that CR is the most critical factor while designing ETC and CR should be focused most followed by N, MFR and WD while designing for ETC.

Variation of daily exergy gain with (a) MFR, (b) N, (c) WD and (d) CR for collector keeping all other parameters persistent has been depicted as Fig. 11. One can see in Fig. 11a that the value of exergy gain decreases as the value of MFR increases. It has been found to occur because fluid flowing through the collector gets lesser time to absorb heat at increased value of MFR and hence increase in temperature is less at increased MFR and hence less exergy output is obtained. One can see in Fig. 11b that the value of exergy gain increases as the value of N is increased because heat collection area increases with the increase in the value of N. One can see in Fig. 11c that the exergy gain for the collector decreases with the increase in water depth because heat is stored as sensible heat in the water kept in the basin. Due to this reason, the temperature of fluid at the inlet of collector is higher resulting in lesser temperature difference between input and output fluid temperatures. It can be seen in Fig. 11d that the value of exergy gain for the collector increases with the increase in the value of CR because more solar energy is focused on the receiver at increased value of CR. The sensitivity of daily exergy gain with regard to (a) MFR, (b) N, (c) WD and (d) CR for collector keeping all other input parameters

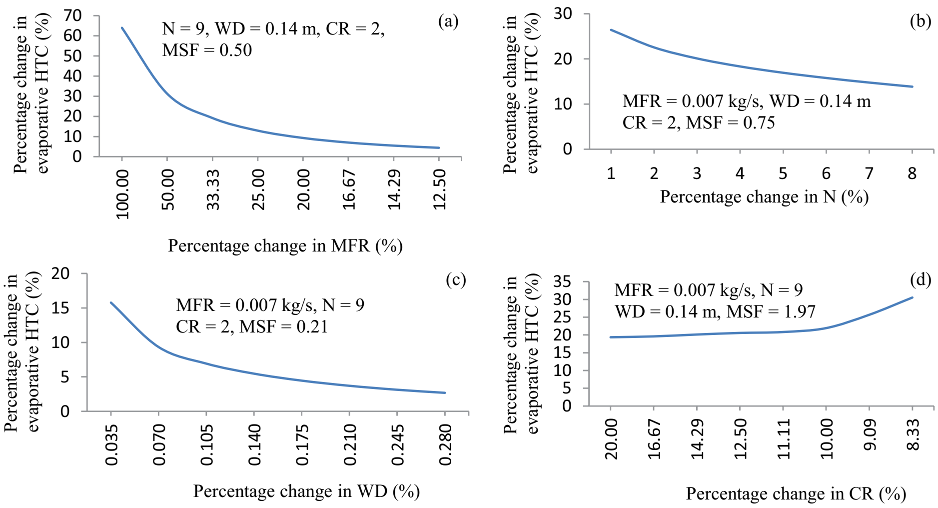

Fig. 10. Sensitivity of daily HTC with regard to (a) MFR, (b) N, (c) WD and (d) CR for NCPCETC-DS maintaining other parameters at the input of system constant.

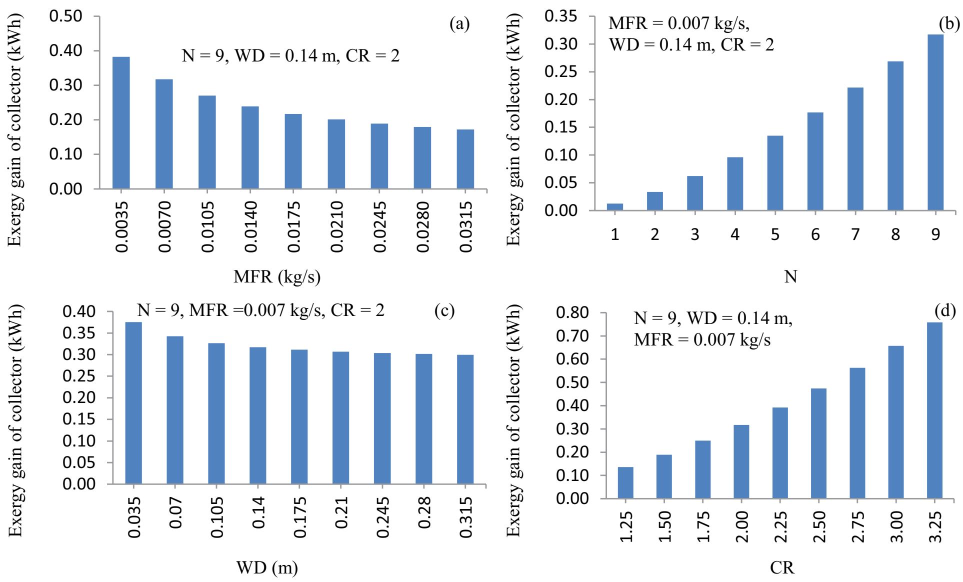

Fig. 11. Dissimilarity of daily exergy gain with (a) MFR, (b) N, (c) WD and (d) CR for collector maintaining other parameters at the input of system constant.

persistent has been depicted as Fig. 12. It is seen in Fig. 12 that the value of sensitivity is higher at higher percentage change in the value of MFR, N, WD and CR due to the similar trends in the slope of curves. The mean value of sensitivity figure (SF) for exergy gain of collector has been estimated to be 1.97, 0.75, 0.49 and 0.21 with respect to CR, N, MFR and WD respectively. It means that CR is the most critical parameter for exergy gain which contribute to output of the system. Hence, CR should be focused most followed by N, MFR and WD from exergy gain viewpoint.

The dissimilarity of daily exergy gain and daily exergy efficiency with MFR at selected values of N, CR and WD for NCPCETC-DS has been revealed as Fig. 13. It can be seen in Fig. 13 that the value of exergy output as well as exergy efficiency decreases as the value of MFR is increased because the fluid flowing through the collector gets less time to absorb heat from solar energy at enhanced value of MFR. The value of exergy output as well as exergy efficiency becomes almost constant beyond 0.021 kg/s because at very high value of MFR, fluid just glides through the tubes without absorbing solar energy due to high velocity of flow. The sensitivity of daily exergy output and daily exergy efficiency with regard to MFR at selected values of N, CR and WD for NCPCETC-DS has been revealed as Fig. 14. It can be seen in Fig. 14 that the sensitivity is higher at higher percentage change in the value of MFR because of similar variation in the slope of the curve.

The dissimilarity of daily exergy gain and daily exergy efficiency with N at selected values of MFR, CR and WD for NCPCETC-DS has been revealed as Fig. 15. It can be seen in Fig. 15 that the value both daily exergy gain and exergy efficiency increases with the increase in the value of N because heat collection area increase with the increase in the value of N. The sensitivity of daily exergy gain and exergy efficiency with regard to N at selected values of N, CR and MFR for NCPCETC-DS has been revealed as Fig. 16. It can be seen in Fig. 16 that the sensitivity is higher at higher percentage change in the value of N due to the similar variation in the slope of curve. The dissimilarity of daily exergy gain and

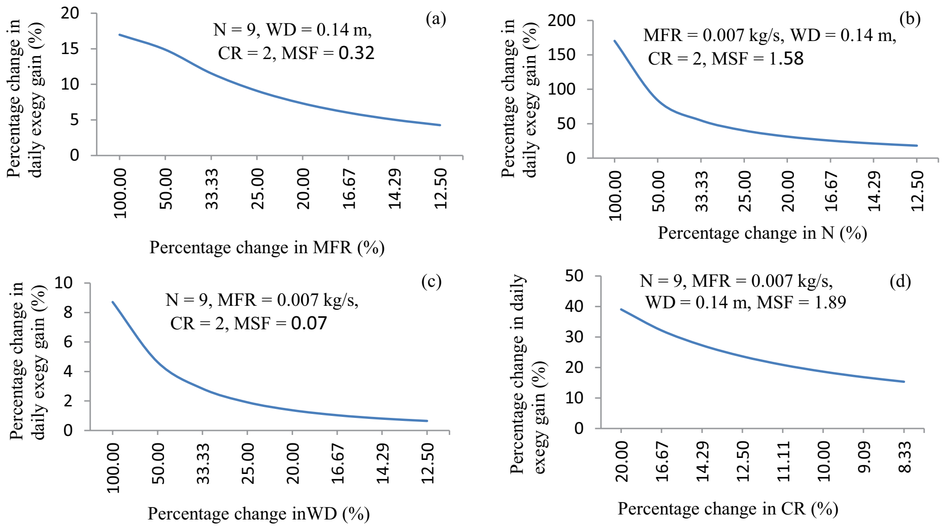

Fig. 12. Sensitivity of daily exergy gain with regard to (a) MFR, (b) N, (c) WD and (d) CR for collector maintaining other parameters at the input of system constant.

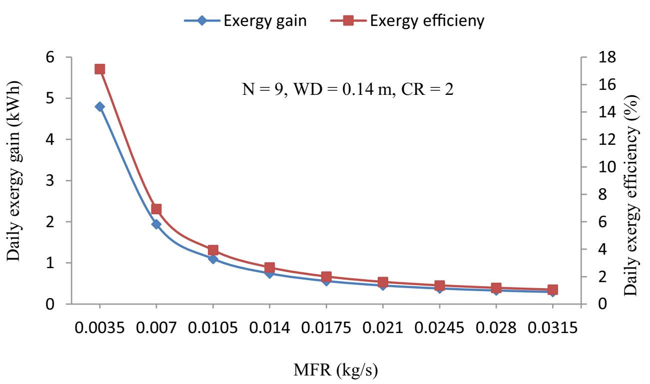

Fig. 13. Dissimilarity of daily exergy gain and daily exergy efficiency with MFR at selected values of N, CR and WD for NCPCETC-DS.

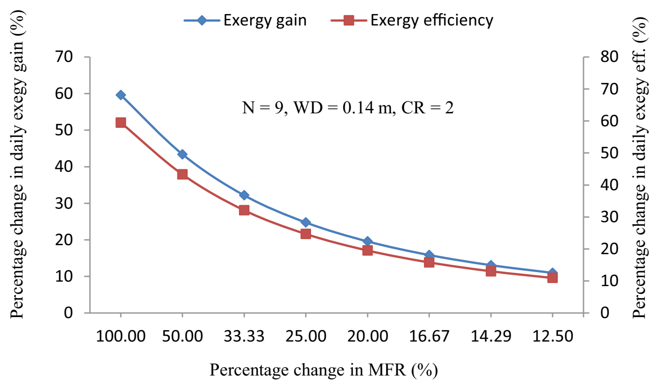

Fig. 14. Sensitivity of daily exergy output and daily exergy efficiency with regard to MFR at selected values of N, CR and WD for NCPCETC-DS.

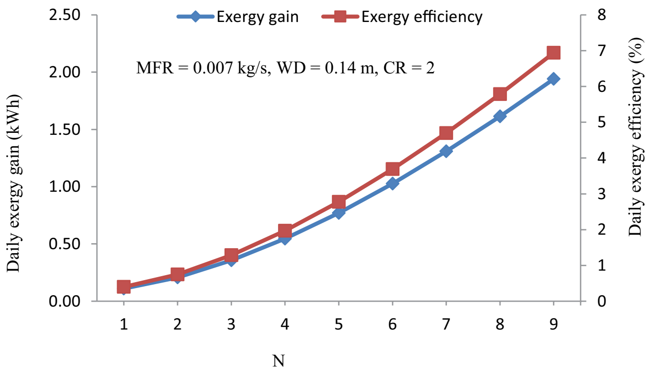

Fig. 15. Dissimilarity of daily exergy gain and daily exergy efficiency with N at selected values of MFR, CR and WD for NCPCETC-DS.

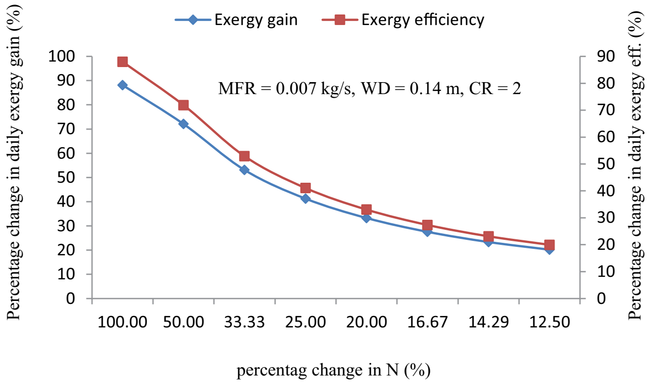

Fig. 16. Sensitivity of daily exergy gain and exergy efficiency with regard to N at selected values of N, CR and MFR for NCPCETC-DS.

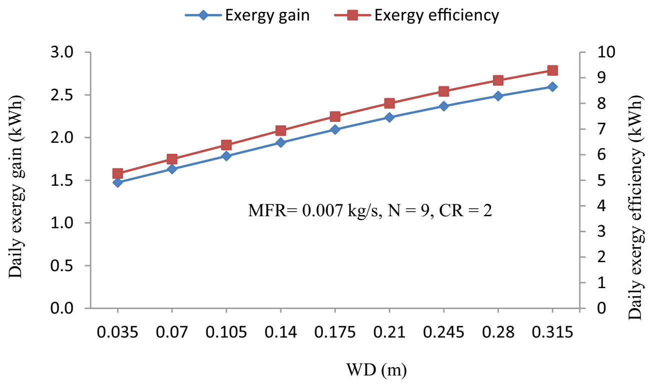

Fig. 17. Dissimilarity of daily exergy gain and daily exergy efficiency with WD at selected values of N, CR and MFR for NCPCETC-DS.

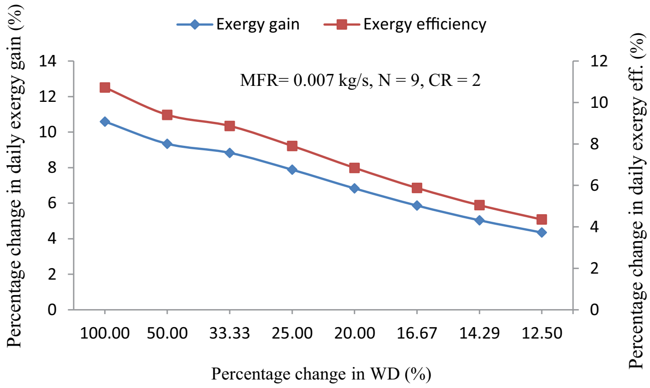

Fig. 18. Sensitivity of daily exergy gain and exergy efficiency with regard to WD at selected values of N, CR and MFR for NCPCETC-DS.

daily exergy efficiency with WD at selected values of N, CR and MFR for NCPCETC-DS has been revealed as Fig. 17. It can be seen in Fig. 17 that the value of exergy output as well as exergy efficiency increases with the increase in the value of WD because more sensible heat is stored at higher WD which further contributes to the exergy output at night. The sensitivity of daily exergy gain and exergy efficiency with regard to WD at selected values of N, CR and MFR for NCPCETC-DS has been revealed as Fig. 18. One can see the percentage change in output at the particular percentage change in the input. The ratio of percentage change in exergy gain/exergy efficiency to the corresponding percentage change in WD gives sensitivity figure. Higher the sensitivity figure, higher is the effect of that input parameter on the output of the system.

The variation of daily exergy gain and exergy efficiency with CR at selected values of N, WD and MFR for NCPCETC-DS has been revealed as Fig. 19. It can be seen in Fig. 19 that the value of both exergy gain and exergy efficiency increase with the increase in the value of CR because more solar energy is focused on the receiver surface at increased value of CR and hence higher heat is added to the basin of solar still which results in the increased value of temperature of water in the basin. The sensitivity of daily exergy gain and exergy efficiency with regard to CR at

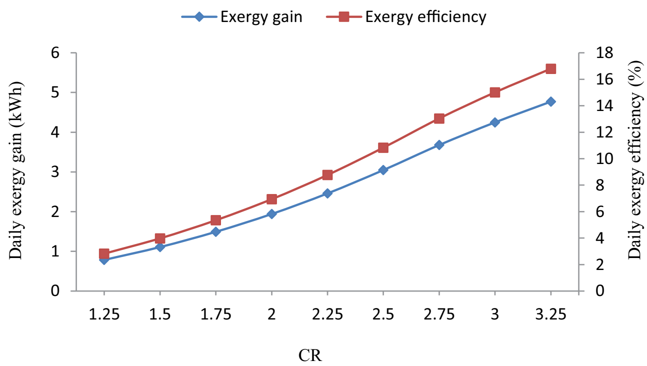

Fig. 19. Dissimilarity of daily exergy gain and exergy efficiency with CR at selected values of N, WD and MFR for NCPCETC-DS.

selected values of N, WD and MFR for NCPCETC-DS has been revealed as Fig. 20. It can be seen in Fig. 20 that the percentage change in output is higher at higher percentage change in CR and vice-versa. One can see the percentage change in output corresponding to the percentage change in input. The ratio of percentage change in exergy output/exergy efficiency to the percentage change in CR will give the value of sensitivity figure. Higher the value of sensitivity figure, higher will be the effect of CR on exergy output/exergy efficiency and vice-versa.

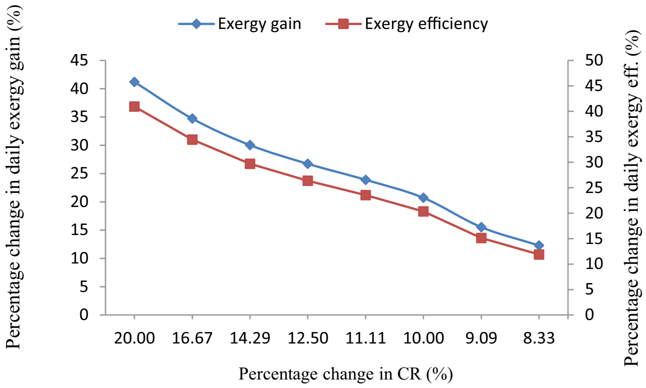

Fig. 20. Sensitivity of daily exergy gain and exergy efficiency with regard to CR at selected values of N, WD and MFR for NCPCETC-DS.

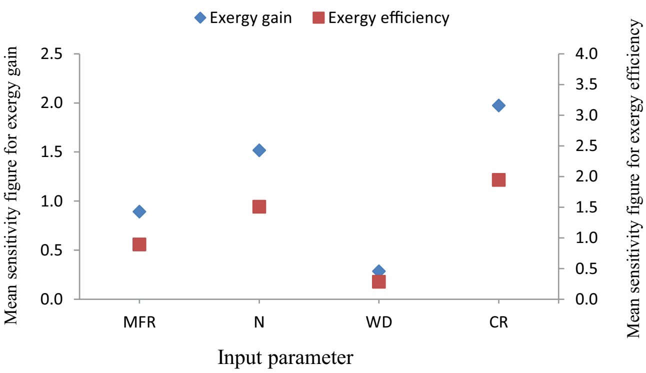

Fig. 21. Comparative sensitivity figure of exergy gain as well as exergy efficiency with respect to input parameter (MFR/N/WD/CR) for NCPCETC-DS.

The comparative sensitivity figure of exergy output as well as exergy efficiency with respect to input parameter (MFR/N/WD/CR) for NCPCETC-DS has been revealed as Fig. 21. One can see in Fig. 21 that the value of sensitivity figure is highest with respect to CR followed by N, MFR and WD. It means that CR is the most critical factor while designing or installing NCPCETC-DS and hence CR should be focused most followed by N, MFR and WD. It can also be seen that the value of sensitivity figure for exergy efficiency of NCPCETC-DS is highest with respect to CR followed by N, MFR and WD. It means that CR is the most critical factor for exergy efficiency of the system and hence CR should be focused most followed by N, MFR and CR while designing such system. The comparative study of the current analysis with earlier published research has been presented as Table 2.

7. Conclusions

The sensitivity analysis of double slope solar still having compound parabolic concentrator integrated ETCs by incorporating heat transfer coefficients, exergy gain and exergy efficiency has been done. The sensitivity study for collectors has been presented. The present investigation can be concluded as follows:

- The value of exergy output for NCPCETCs diminishes with the increase in the value of MFR and WD; however, value of exergy output for NCPCETCs increases with the increase in the value of N and CR. The mean value of SF for NCPCETCs has been estimated to be 1.97, 0.75, 0.49 and 0.21 with respect to CR, N, MFR and WD respectively.
- Values of HTCs diminishes with the increase in the value of MFR; however, value of HTCs increases with the increase in CR, N and WD. The mean value of SF for evaporative HTCs of NCPCETC-DS is estimated to be 1.88, 1.58, 0.32 and 0.07 with respect to CR, N, MFR and WD respectively.
- Value of exergy gain as well as exergy efficiency of the

Table 2
Comparative study of sensitivity analysis using OAT technique

System	Analysis	Remarks
DS integrated NCPCETCs (Current study)	Sensitivity analysis using OAT technique	Highest value of SF for exergy output has been obtained as 1.973 w.r.t. CR. Also, the highest value of SF for exergy efficiency has been obtained as 1.943 w.r.t. CR.
DS integrated with PVT concentrator collectors [28]	Sensitivity analysis using OAT technique	Analysis was done for potable water yield and electric power.
DS integrated with PVTFPCs [29]	Sensitivity analysis using OAT technique	Highest value of SF for water yield was found as 0.195 with respect to WD.
DS integrated with ETCs [30]	Sensitivity analysis using OAT technique	Highest value of SF for potable water yield was found as 0.68 with respect to N. Also, value of SF for exergy output was highest as 1.4 w.r.t N.
Single slope solar still integrated with ETCs [31]	Sensitivity analysis using OAT technique	Highest value of SF for potable water yield was found as 0.74 with respect to inclination of collector. Also, value of SF for exergy output was highest as 1.31 w.r.t N.

system diminishes with the increase in the value of MFR; however, value of exergy output as well as exergy efficiency diminishes with the increase in the value of MFR, N and CR. The mean value of sensitivity figure for exergy output has been found to be 1.973, 1.532, 0.904 and 0.2986 with respect to CR, N, MFR and WD respectively. The mean value of sensitivity figure for exergy efficiency has been found to be 1.943, 1.526, 0.902 and 0.287 with respect to CR, N, MFR and WD respectively.

- The mean value of SF of exergy for collector and NCPCETC-DS has been found to be highest with respect to CR followed by N, MFR and WD. Also, the mean value of SF of exergy efficiency for NCPCETC-DS has been found to be highest with respect to CR followed by N, MFR and WD.

8. Recommendations

The outcome of this work will help the designer and installer of double slope solar still working in active mode by providing the feedback on the effect of various input parameters on the output by incorporating exergy. They will have the information regarding which parameter is going to affect the output most and accordingly they will be in a position to decide as which parameter is to be focused more. The solar energy operated water purifier of double slope type working in active mode has not been tested experimentally. So, authors recommend its experimental validation before the actual installation as solar energy operated water purifier plant. The sensitivity analysis can be carried out using other techniques like an artificial neural network and a multiple linear regression model and results obtained can be verified with the results reported in this article. The authors plan to extend this research to include geographic and weather variations in future research.

Symbols

A_b	—	Area of basin, m^2
A_g	—	Area of glass cover, m^2
C	—	Specific heat capacity, J/kg-K
CPC	—	Compound parabolic concentrator
CR	—	Concentration ratio
DS	—	Double slope solar still
F'	—	Collector efficiency factor, dimensionless
$\dot{E}x$	—	Hourly exergy gain
ETC	—	Evacuated tubular collector
HTC	—	Heat transfer coefficient
h_{cwg}	—	Convective HTC from water to inner surface of glass cover, W/m^2-K
h_{ewg}	—	Evaporative HTC from water surface to inner surface of glass cover, W/m^2-K
h_{ba}	—	HTC from blackened surface to water mass, W/m^2-K
h_{bw}	—	HTC from blackened surface to water mass, W/m^2-K
h_{rwg}	—	Radiative HTC from water surface to inner surface of glass cover, W/m^2-K
h_r	—	Radiative HTC, W/m^2-K
h_{1w}	—	Total HTC from water surface to inner surface of glass cover, W/m^2-K
h_{1g}	—	Total HTC from outer surface of glass cover facing to ambient, W/m^2-K
$I(t)$	—	Solar intensity on collector, W/m^2
$I_S(t)$	—	Solar intensity on glass cover of solar still, W/m^2
K	—	Thermal conductivity, W/m-K
L_g	—	Thickness of glass, m
L	—	Latent heat, J/kg
L'	—	Length, m
MFR/$\dot{m}_f$	—	Mass flow rate of fuid/water, kg/s
N	—	Number of collectors
NCPCETC-DS	—	Solar still of DS type included with N similar CPCETCs having series connection
PF_c	—	Penalty factor due to the glass covers for the glazed portion
PF_1	—	Penalty factor first, dimensionless
PF_2	—	Penalty factor second, dimensionless
PW	—	Potable water
SA	—	Sensitivity analysis
SF	—	Sensitivity figure
SEBWP	—	Solar energy based water purifier
T_{foN}	—	Outlet water temperature at the end of Nth water collector, °C
T_a	—	Ambient air temperature, °C
T_{gi}	—	Glass temperature at inner surface of glass cover, °C
t	—	Time, h
T_{wo}	—	Water temperature at $t = 0$, °C
T_w	—	Water temperature, °C
U_L	—	Overall heat transfer coefficient, W/m^2-K
V	—	Velocity of air, m/s
WD	—	water depth

Subscripts

eff	—	Effective
ex	—	Exergy
f	—	Fluid
g	—	Glass
in	—	Incoming
out	—	Outgoing
w	—	Water

Greek

α	—	Absorptivity (fraction)
η	—	Efficiency, %
$(\alpha\tau)_{eff}$	—	Product of effective absorptivity and transmittivity
σ	—	Stefan–Boltzmann constant, W/m^2-K^4
τ	—	Transmittivity

References

[1] S.N. Rai, G.N. Tiwari, Single basin solar still coupled with flat plate collector, Energy Convers. Manage., 23 (1983) 145–149.

[2] S. Kumar, A. Tiwari, An experimental study of hybrid photovoltaic thermal (PV/T)-active solar still, Int. J. Energy Res., 32 (2008) 847–858.

[3] E.C. Kern Jr., M.C. Russell, Combined Photovoltaic and Thermal Hybrid Collector Systems, Conference: IEEE Photovoltaic Specialists Conference, Washington, DC, USA, 5 June 1978, pp. 1153–1157.

[4] G. Singh, S. Kumar, G.N. Tiwari, Design, fabrication and performance evaluation of a hybrid photovoltaic thermal (PVT) double slope active solar still, Desalination, 277 (2011) 399–406.
[5] D.B. Singh, J.K. Yadav, V.K. Dwivedi, S. Kumar, G.N. Tiwari, I.M. Al-Helal, Experimental studies of active solar still integrated with two hybrid PVT collectors, Sol. Energy, 130 (2016) 207–223.
[6] G.N. Tiwari, J.K. Yadav, D.B. Singh, I.M. Al-Helal, A.M. Abdel-Ghany, Exergoeconomic and enviroeconomic analyses of partially covered photovoltaic flat plate collector active solar distillation system, Desalination, 367 (2015) 186–196.
[7] D.B. Singh, G.N. Tiwari, Enhancement in energy metrics of double slope solar still by incorporating N identical PVT collectors, Sol. Energy, 143 (2017) 142–161.
[8] D.B. Singh, Exergoeconomic and enviroeconomic analyses of N identical photovoltaic thermal integrated double slope solar still, Int. J. Exergy, 23 (2017) 347–366.
[9] D.B. Singh, N. Kumar, Harender, S. Kumar, S.K. Sharma, A. Mallick, Effect of depth of water on various efficiencies and productivity of N identical partially covered PVT collectors incorporated single slope solar distiller unit, Desal. Water Treat., 138 (2019) 99–112.
[10] D.B. Singh, Improving the performance of single slope solar still by including N identical PVT collectors, Appl. Therm. Eng., 131 (2018) 167–179.
[11] D.B. Singh, N. Kumar, S. Kumar, V.K. Dwivedi, J.K. Yadav, G.N. Tiwari, Enhancement in exergoeconomic and enviroeconomic parameters for single slope solar still by incorporating N identical partially covered photovoltaic collectors, J. Sol. Energy Eng. Trans. ASME, 140 (2018) 051002 (18 pages).
[12] L. Sahota, G.N. Tiwari, Exergoeconomic and enviroeconomic analyses of hybrid double slope solar still loaded with nanofluids, Energy Convers. Manage., 148 (2017) 413–430.
[13] F. Carranza, C. Villa, J. Aguilara, H.A. Borbón-Nuñez, D. Sauceda, Experimental study on the potential of combining TiO_2, ZnO, and Al_2O_3 nanoparticles to improve the performance of a double-slope solar still equipped with saline water preheating, Desal. Water Treat., 216 (2021) 14–33.
[14] M.R. Kouadri, N. Chennouf, M.H. Sellami, M.N. Raache, A. Benarima, The effective behavior of ZnO and CuO during the solar desalination of brackish water in southern Algeria, Desal. Water Treat., 218 (2021) 126–134.
[15] A.W. Kandeal, N.M. El-Shafai, M.R. Abdo, A.K. Thakur, I.M. El-Mehasseb, I. Maher, M. Rashad, A.E. Kabeel, N. Yang, S.W. Sharshir, Improved thermo-economic performance of solar desalination via copper chips, nanofluid, and nano-based phase change material, Sol. Energy, 224 (2021) 1313–1325.
[16] A.K. Thakur, R. Sathyamurthy, R. Velraj, R. Saidur, I. Lynch, R. Venkatesh, P.G. Kumar, S.C. Kim, M. Sillanpää, A novel solar absorber using activated carbon nanoparticles synthesized from bio-waste for the performance improvement of solar desalination unit, Desalination, 527 (2022) 115564, doi: 10.1016/j.desal.2022.115564.
[17] P.K. Tyagi, R. Kumar, Z. Said, Recent advances on the role of nanomaterials for improving the performance of photovoltaic thermal systems: trends, challenges and prospective, Nano Energy, 93 (2022) 106834, doi: 10.1016/j.nanoen.2021.106834.
[18] D. Atheaya, A. Tiwari, G.N. Tiwari, I.M. Al-Helal, Analytical characteristic equation for partially covered photovoltaic thermal (PVT) – compound parabolic concentrator (CPC), Sol. Energy, 111 (2015) 176–185.
[19] R. Tripathi, G.N. Tiwari, I.M. Al-Helal, Thermal modelling of N partially covered photovoltaic thermal (PVT)–compound parabolic concentrator (CPC) collectors connected in series, Sol. Energy, 123 (2016) 174–184.
[20] D.B. Singh, G.N. Tiwari, Performance analysis of basin type solar stills integrated with N identical photovoltaic thermal (PVT) compound parabolic concentrator (CPC) collectors: a comparative study, Sol. Energy, 142 (2017) 144–158.
[21] D.B. Singh, G.N. Tiwari, Exergoeconomic, enviroeconomic and productivity analyses of basin type solar stills by incorporating N identical PVT compound parabolic concentrator collectors: a comparative study, Energy Convers. Manage., 135 (2017) 129–147.
[22] D.B. Singh, G.N. Tiwari, Effect of energy matrices on life cycle cost analysis of partially covered photovoltaic compound parabolic concentrator collector active solar distillation system, Desalination, 397 (2016) 75–91.
[23] V.S. Gupta, D.B. Singh, R.K. Mishra, S.K. Sharma, G.N. Tiwari, Development of characteristic equations for PVT-CPC active solar distillation system, Desalination, 445 (2018) 266–279.
[24] V.S. Gupta, D.B. Singh, S.K. Sharma, N. Kumar, T.S. Bhatti, G.N. Tiwari, Modeling self-sustainable fully-covered photovoltaic thermal-compound parabolic concentrators connected to double slope solar distiller, Desal. Water Treat., 190 (2020) 12–27.
[25] V. Singh, D.B. Singh, N. Kumar, R. Kumar, Effect of number of collectors (N) on life cycle conversion efficiency of single slope solar desalination unit coupled with N identical partly covered compound parabolic concentrator collectors, Mater. Today:. Proc., 28 (2020) 2185–2189.
[26] D.B. Singh, G. Singh, N. Kumar, P.K. Singh, R. Kumar, Effect of mass flow rate on energy payback time of single slope solar desalination unit coupled with N identical compound parabolic concentrator collectors, Mater. Today:. Proc., 28 (2020) 2551–2556.
[27] G.K. Sharma, N. Kumar, D.B. Singh, A. Mallick, Exergoeconoic analysis of single slope solar desalination unit coupled with PVT-CPCs by incorporating the effect of dissimilarity of the rate of flowing fluid mass, Mater. Today:. Proc., 28 (2020) 2364–2368.
[28] H. Prasad, P. Kumar, R.K. Yadav, A. Mallick, N. Kumar, D.B. Singh, Sensitivity analysis of N identical partially covered (50%) PVT compound parabolic concentrator collectors integrated double slope solar distiller unit, Desal. Water Treat., 153 (2019) 54–64.
[29] K. Bharti, S. Manwal, C. Kishore, R.K. Yadav, P. Tiwar, D.B. Singh, Sensitivity analysis of N alike partly covered PVT flat plate collectors integrated double slope solar distiller unit, Desal. Water Treat., 211 (2021) 45–59.
[30] D.B. Singh, Sensitivity analysis of N identical evacuated tubular collectors integrated double slope solar distiller unit by incorporating the effect of exergy, Int. J. Exergy, 34 (2021) 424–447.
[31] A. Raturi, D.B. Singh, P.P. Patil, A.K. Sharma, Sensitivity analysis of a solar still of a single slope type included with N similar evacuated tubular collectors having series connection, Desal. Water Treat., 234 (2021) 309–323.
[32] A. Raturi, R. Dobriyal, R.K. Sharma, A. Dwivedi, S.P. Singh, D.B. Singh, Sensitivity investigation for solar still of double slope type included with N similar CPC integrated ETC by incorporating yield and efficiency, Desal. Water Treat., 244 (2021) 12–26.
[33] K. Sampathkumar, T.V. Arjunan, P. Senthilkumar, The experimental investigation of a solar still coupled with an evacuated tube collector, Energy Sources Part A, 35 (2013) 261–270.
[34] R.V. Singh, S. Kumar, M.M. Hasan, M.E. Khan, G.N. Tiwari, Performance of a solar still integrated with evacuated tube collector in natural mode, Desalination, 318 (2013) 25–33.
[35] S. Kumar, A. Dubey, G.N. Tiwari, A solar still augmented with an evacuated tube collector in forced mode, Desalination, 347 (2014) 15–24.
[36] R.K. Mishra, V. Garg, G.N. Tiwari, Energy matrices of U-shaped evacuated tubular collector (ETC) integrated with compound parabolic concentrator (CPC), Sol. Energy, 153 (2017) 531–539.
[37] D.B. Singh, V.K. Dwivedi, G.N. Tiwari, N. Kumar, Analytical characteristic equation of N identical evacuated tubular collectors integrated single slope solar still, Desal. Water Treat., 88 (2017) 41–51.
[38] D.B. Singh, G.N. Tiwari, Analytical characteristic equation of N identical evacuated tubular collectors integrated double slope solar still, J. Sol. Energy Eng., 135 (2017) 051003 (11 pages).
[39] D.B. Singh, G.N. Tiwari, Energy, exergy and cost analyses of N identical evacuated tubular collectors integrated basin type solar stills: a comparative study, Sol. Energy, 155 (2017) 829–846.

[40] R.J. Issa, B. Chang, Performance study on evacuated tubular collector coupled solar still in west Texas climate, Int. J. Green Energy, 14 (2017) 793–800.
[41] D.B. Singh, I.M. Al-Helal, Energy metrics analysis of N identical evacuated tubular collectors integrated double slope solar still, Desalination, 432 (2018) 10–22.
[42] D.B. Singh, N. Kumar, A. Raturi, G. Bansal, A. Nirala, N. Sengar, Effect of Flow of Fluid Mass Per Unit Time on Life Cycle Conversion Efficiency of Double Slope Solar Desalination Unit Coupled with N Identical Evacuated Tubular Collectors, Lecture Notes in Mechanical Engineering, Advances in Manufacturing and Industrial Engineering, Select Proceedings of ICAPIE 2019, 2021, pp. 393–402.
[43] S.K. Sharma, D.B. Singh, A. Mallick, S.K. Gupta, Energy metrics and efficiency analyses of double slope solar distiller unit augmented with N identical parabolic concentrator integrated evacuated tubular collectors: a comparative study, Desal. Water Treat., 195 (2020) 40–56.
[44] S.K. Sharma, A. Mallick, S.K. Gupta, N. Kumar, D.B. Singh, G.N. Tiwari, Characteristic equation development for double slope solar distiller unit augmented with N identical parabolic concentrator integrated evacuated tubular collectors, Desal. Water Treat., 187 (2020) 178–194.
[45] S.W. Sharshir, A.H. Elsheikh, Y.M. Ellakany, A.W. Kandeal, E.M.A. Edreis, R. Sathyamurthy, A.K. Thakur, M.A. Eltawil, M.H. Hamed, A.E. Kabeel Improving the performance of solar still using different heat localization materials, Environ. Sci. Pollut. Res., 27 (2020) 12332–12344.
[46] A.K. Thakur, R. Sathyamurthy, S.W. Sharshir, A.E. Kabeel, M.R. Elkadeem, Z. Ma, A.M, Manokar, M. Arıcı, A.K. Pandey, R. Saidur, Performance analysis of a modified solar still using reduced graphene oxide coated absorber plate with activated carbon pellet, Sustain. Energy Technol. Asses., 45 (2021) 101046.
[47] R.V. Patel, K. Bharti, G. Singh, R. Kumar, S. Chhabra, D.B. Singh, Solar still performance investigation by incorporating the shape of basin liner: a short review, Mater. Today:. Proc., 43 (2021) 597–604.
[48] R.V. Patel, K. Bharti, G. Singh, G. Mittal, D.B. Singh, A. Yadav, Comparative investigation of double slope solar still by incorporating different types of collectors: a mini review, Mater. Today:. Proc., 38 (2021) 300–304.
[49] R.V. Patel, G. Singh, K. Bharti, R. Kumar, D.B. Singh, A mini review on single slope solar desalination unit augmented with different types of collectors, Mater. Today:. Proc., 38 (2021) 204–210.
[50] G. Singh, D.B. Singh, S. Kumara, K. Bharti, S. Chhabra, A review of inclusion of nanofluids on the attainment of different types of solar collectors, Mater. Today:. Proc., 38 (2021) 153–159.
[51] G. Bansal, D.B. Singh, C. Kishore, V. Dogra, Effect of absorbing material on the performance of solar still: a mini review, Mater. Today:. Proc., 26 (2020) 1884–1887.
[52] A. Mourad, A. Aissa, Z. Said, O. Younis, M. Iqbal, A. Alazzam, Recent advances on the applications of phase change materials for solar collectors, practical limitations, and challenges: a critical review, J. Energy Storage, 49 (2022) 104186, doi: 10.1016/j.est.2022.104186.
[53] Z. Said, A.A. Hachicha, S. Aberoumand, B.A.A. Yousef, E.T. Sayed, E. Bellos, Recent advances on nanofluids for low to medium temperature solar collectors: energy, exergy, economic analysis and environmental impact, Prog. Energy Combust. Sci., 84 (2021) 100898, doi: 10.1016/j.pecs.2020.100898.
[54] P. Shankar, A. Dubey, S. Kumar, G.N. Tiwari, Production of clean water using ETC integrated solar stills: thermoenviroeconomic assessment, Desal. Water Treat., 218 (2021) 106–118.
[55] S. Abdallah, M. Nasir, D. Afaneh, Performance evaluation of spherical and pyramid solar stills with chamber stepwise basin, Desal. Water Treat., 218 (2021) 119–125.
[56] S.K. Sharma, A. Mallick, D.B. Singh, G.N. Tiwari, Experimental study of solar energy–based water purifier of single-slope type by incorporating a number of similar evacuated tubular collectors, Environ. Sci. Pollut. Res., 29 (2022) 6837–6856.
[57] D. Purnachandrakumar, G. Mittal, R.K. Sharma, D.B. Singh, S. Tiwari, H. Sinhmar, Review on performance assessment of solar stills using computational fluid dynamics (CFD), Environ. Sci. Pollut. Res., 29 (2022) 38673–38714.
[58] R. Kumar, D.B. Singh, A. Dewangan, V.K. Singh, N. Kumar, Performance of evacuated tube solar collector integrated solar desalination unit — a review, Desal. Water Treat., 230 (2021) 92–115.
[59] D. Kumar, R.K. Sharma, D.B. Singh, Effect of variation of mass-flow-rate and number of collectors on performance of active solar still, Desal. Water Treat., 248 (2022) 1–17.
[60] R.K. Yadav, M. Kumar, J. Singh D.B. Singh, N. Kumar, Effects of the dissimilarity of water depth on energy and exergy efficiencies and productivity of solar energy, Int. J. Exergy, 38 (2022) 333–345.
[61] V. Singh, R. Kumar, D.B. Singh, An investigation on effect of dissimilarity of mass flow rate on hourly, daily and annual efficiencies of double slope type solar still included with N similar PVT compound parabolic concentrators, Desal. Water Treat., 246 (2022) 36–53.
[62] D.B. Singh, D. Kumar, R.K. Yadav, S. K, Sharma, Y. Chaturbedi, N. Kumar, V.K. Dwivedi, An investigation of effect of mass flow rate variation on productivity, exergoeconomic and enviroeconomic parameters of N similar PVTCPCs included with double slope solar still, Desal. Water Treat., 243 (2021) 1–17.
[63] D.B. Singh, R.K. Yadav, Y. Chaturvedi, M. Kumar, G.K. Sharma, N. Kumar, Study on effect of dissimilarity of mass flow rate on energy metrics of solar energy-based double slope water purifier by incorporating N alike PVT compound parabolic concentrator collectors, Desal. Water Treat., 231 (2021) 27–43.
[64] A.K. Thakur, R. Sathyamurthy, Improving the potable water generation through tubular solar still using eggshell powder (bio-based energy source) as a natural energy storage material – an experimental approach, Environ. Sci. Pollut. Res., 29 (2022) 40903–40920.
[65] P.K. Nag, Basic and Applied Thermodynamics, Tata McGraw-Hill, NY, 2004.
[66] D.M. Hamby, A review of techniques for parameter sensitivity analysis of environmental model, Environ. Monit. Assess., 32 (1994) 135–154.
[67] A. Saltelli, P. Annoni, How to avoid a perfunctory sensitivity analysis, Environ. Modell. Software, 25 (2010) 1508–1517.
[68] W. Ajbar, A. Parrales, S. Silva-Martínez, A. Bassam, O.A. Jaramillo, J.A. Hernández, Identification of the relevant input variables for predicting the parabolic trough solar collector's outlet temperature using an artificial neural network and a multiple linear regression model, J. Renewable Sustainable Energy, 13 (2021) 043701, doi: 10.1063/5.0055992.
[69] W. Ajbar, A. Parrales, A. Huicochea, J.A. Hernández, Different ways to improve parabolic trough solar collectors' performance over the last four decades and their applications: a comprehensive review, Renewable Sustainable Energy Rev., 156 (2022) 111947, doi: 10.1016/j.rser.2021.111947.